Nonclassical correlations between terahertz-bandwidth photons mediated by rotational quanta in hydrogen molecules

Bustard, Philip J.; Erskine, Jennifer; England, Duncan G.; Nunn, Josh; Hockett, Paul; Lausten, Rune; Spanner, Michael; Sussman, Benjamin J.

Publisher's version / Version de l'éditeur:
https://doi.org/10.1364/OL.40.000922
Optics Letters, 40, 6, pp. 922-925, 2015-03-15

Nonclassical correlations between terahertz-bandwidth photons mediated by rotational quanta in hydrogen molecules

Philip J. Bustard,[1] Jennifer Erskine,[1] Duncan G. England,[1] Josh Nunn,[1,2] Paul Hockett,[1] Rune Lausten,[1] Michael Spanner,[1] and Benjamin J. Sussman[1,2,*]

[1]*National Research Council of Canada, 100 Sussex Drive, Ottawa, Ontario, K1A 0R6, Canada*

[2]*Department of Physics, University of Ottawa, Ottawa, Ontario, K1N 6N5, Canada*

**Corresponding author: ben.sussman@nrc.ca*

Received December 17, 2014; revised January 23, 2015; accepted January 26, 2015; posted January 28, 2015 (Doc. ID 230953); published March 4, 2015

Quantum photonics offers much promise for the development of new technologies. The ability to control the interaction of light and matter at the level of single quantum excitations is a prerequisite for the construction of potentially powerful devices. Here we use the rotational levels of a room temperature ensemble of hydrogen molecules to couple two distinct optical modes at the single photon level using femtosecond pulses with 2 THz bandwidth. We observe photon correlations that violate a Cauchy–Schwarz inequality, thereby verifying the creation of a nonclassical state. This work demonstrates the rich potential of molecules for use in ultrafast quantum photonic devices.

OCIS codes: (020.1670) Coherent optical effects; (320.7110) Ultrafast nonlinear optics; (290.5860) Scattering, Raman; (270.1670) Coherent optical effects.

http://dx.doi.org/10.1364/OL.40.000922

Nonclassical physics is a prevalent theme in several areas of current photonic technology research. Example applications include single photon sources [1], cryptographic key generation [2], and the drive to implement optical quantum computing [3]. Nonlinear quantum optical phenomena are powerful tools for the development of such technologies: they enable the interaction of multiple photons, mediated by dipole coupling to levels in atomic, ionic, solid-state, and molecular systems. For example, a variety of nonlinear phenomena including electromagnetically induced transparency [4], photon echoes [5,6], and Raman scattering [7], have been used to build optical quantum memories [8], which act as temporary buffers for photonic quantum information.

In ensemble quantum memories [9,10], the level structure and internal states of the storage system must be suited to the frequency and bandwidth of the stored photons. Furthermore, the memory lifetime for high-fidelity storage must be sufficiently long for a desired application. Memories for use in long-distance quantum communication require correspondingly long storage times [11,12]; memories designed for this purpose are therefore generally implemented in those atomic ensembles and ion-doped crystals that exhibit prolonged coherence and can store MHz–GHz bandwidth photons [7,13–20]. For compact photonic processing on the meter scale, operational speed is another salient parameter: large processing potential can be obtained by effecting multiple operations in quick succession.

We recently demonstrated that a room temperature ensemble of molecules can be used as a coherent absorptive photonic memory by storing and retrieving coherent femtosecond pulses with terahertz (THz) bandwidth using a collective vibrational coherence in hydrogen gas [21]. In this Letter we show that THz-bandwidth quantum-level operation of a DLCZ emissive quantum memory [22] is possible using collective rotational coherence in a room temperature ensemble of hydrogen molecules. We verify the production of nonclassical photon correlations by measuring the violation of a Cauchy–Schwarz inequality. At present, THz-bandwidth manipulations of highly nonclassical photon states are nontrivial because of noise and bandwidth limitations in many systems. This work is important for future quantum photonic devices because it demonstrates the viability of such operations using the internal dynamics of molecules.

The DLCZ emissive memory protocol [22] has been demonstrated in a variety of systems, including atomic ensembles [23–27] and bulk diamond [28]. We use hydrogen molecules with the relevant level structure shown in Figs. 1(a) and 1(b), where the ground state $|g\rangle$ and excited state $|e\rangle$ are rotational states coupled by Raman scattering in a Λ-level scheme; a diagram of our experimental setup is shown in Fig. 1(c). A delocalized rotational quantum (DRQ) is written into an ensemble by spontaneous Stokes Raman scattering using a *write* pulse, and heralded by the detection of a Stokes photon [see Fig. 1(a)]. The DRQ is subsequently annihilated by anti-Stokes Raman scattering, upon application of a *read* pulse, which creates an anti-Stokes photon [see Fig. 1(b)]. Photon correlations can be observed between the Stokes and anti-Stokes fields because they are coupled via the DRQ.

Hydrogen is a homonuclear, diatomic, linear molecule; its rovibrational levels are labeled by the vibrational quantum number v and rotational quantum number J. Each J-level is $(2J+1)$ degenerate with projections $M = -J, -J+1, \ldots, J-1, J$ along the quantization axis. The selection rules for rotational Raman transitions are $\Delta J = \pm 2$ and $\Delta M = 0, \pm 2$. At room temperature, hydrogen's population is distributed between the rotational levels, $J = 0, 1, 2, 3$ of the $v = 0$ vibrational level [29]. Due to the rotational level spacings and the equilibrium 3:1 ratio of *ortho*-:*para*-hydrogen dictated by nuclear spin statistics, 66% of the population resides in the $J = 1$ level. The

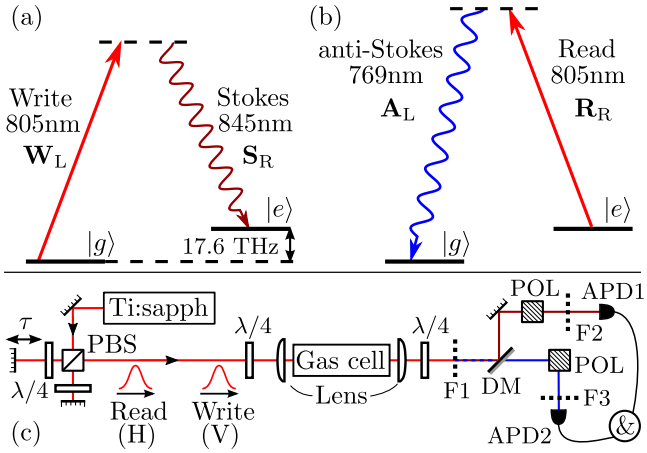

Fig. 1. (a) Right-circular polarized ($\mathbf{S}_R$) Stokes photons are created by spontaneous Raman scattering from the left-circular polarized ($\mathbf{W}_L$) write pulse, with rotational population transfer from $|g\rangle \rightarrow |e\rangle$. (b) Left-circular polarized anti-Stokes photons ($\mathbf{A}_L$) are created by Raman scattering from the right-circular polarized read pulse ($\mathbf{R}_R$); commensurate population completes the $|e\rangle \rightarrow |g\rangle$ transition. (c) Write and read pulses of duration 150 fs are generated using an 80 MHz repetition rate, 3.7 W Ti:sapphire oscillator (Ti:sapph) centered at 805 nm. We reduce the full width at half-maximum bandwidth of the laser output to 2 THz by spectral filtering. The beam is subsequently split using a polarizing beamspliter (PBS); orthogonal linearly polarized write (V-polarized) and read (H-polarized) pulses are recombined with a variable delay τ. The write and read pulses are converted to left-circular ($\mathbf{W}_L$) and right-circular ($\mathbf{R}_R$) polarization, respectively, using a quarter-wave plate ($\lambda/4$) and focussed collinearly using an $f = 50$ mm singlet, into a 7 cm cell filled with hydrogen at pressure $p = 18$ bar and temperature $T = 295$ K. The output light is collimated using an $f = 75$ mm singlet and converted back to linear polarization using an achromatic quarter-wave plate ($\lambda/4$). Pump radiation is separated from rotational Raman Stokes and anti-Stokes photons using notch filter F1. Stokes photons are partitioned from anti-Stokes photons using a dichroic mirror (DM). H-polarized Stokes photons are transmitted at a polarizer (POL), spectrally filtered by filter F2, coupled into a single mode fiber, and detected using an avalanche photodiode (APD1); V-polarized anti-Stokes photons are reflected at a polarizer, spectrally filtered by filter F3, coupled into a single mode fiber, and detected using APD2. Detection events are recorded using a coincidence counting module (&).

strongest spontaneous rotational Raman scattering is therefore on the $J = 1 \rightarrow 3$ transition, with frequency separation of $\nu = 17.6$ THz [29,30]. We use the 3-fold degenerate $(J = 1, M)$ states as the ground level and the corresponding $(J = 3, M + 2)$ states as the excited level. Thus, all three transitions occur simultaneously and independently. Stokes and anti-Stokes photons from this transition are separated from other rotational sidebands using filters F2 and F3, respectively.

Rotational Raman scattering is polarization-dependent, and the coupling is strongest between opposite circular polarizations for the two fields involved [31]. With the propagation direction taken along the quantization axis, this corresponds to the $\Delta M = \pm 2$ transitions; transitions with $\Delta M = 0$ correspond to no change in polarization between the input photons and the scattered photons. The contrast between opposite polarizations for circular polarization write/read pulses means that polarization can be used to label the pulses for time-gating. For left-circular polarized input write pulses $\mathbf{W}_L$, we measured a $\mathbf{S}_L$:$\mathbf{S}_R$ polarization contrast of 1:5.7 in the number of detected Stokes photons, where $\mathbf{S}_L$ ($\mathbf{S}_R$) denote the left- (right-) circular Stokes modes. We measured a $\mathbf{A}_L$:$\mathbf{A}_R$ polarization contrast of 1:5.0 in the number of detected anti-Stokes photons, where $\mathbf{A}_L$ ($\mathbf{A}_R$) denote the left- (right-) circular anti-Stokes modes. These ratios compare favorably with the expected theoretical ratio of 1:6 [31]; discrepancies between the theoretical and measured values can be attributed to pressure-induced birefringence in the cell windows and imperfect phase compensation by the achromatic waveplate.

Nonclassical correlations occur in the spontaneous scattering regime where the probability of scattering more than one photon per pulse is low. At the maximum write pulse energy of $\mathcal{E}_w = 14$ nJ ($\mathcal{N}_w \approx 5.7 \times 10^{10}$ photons), we measure a "singles rate" of $P_S^m = 2.29(5) \times 10^{-4}$ for the probability per pulse of detecting a Stokes photon; the corresponding probability for anti-Stokes scattering from thermal population by the read pulse is $P_A^m = 2.5(1) \times 10^{-5}$. The theoretical probability for Stokes scattering by the write pulse into the solid angle $\Delta\Omega$ of the collimating lens can be estimated using

$$P_S^{th} = NL\mathcal{N}_w\sigma'\Delta\Omega,$$

where $\mathcal{N}_w$ is specified in photon number, N is the number density in state $|g\rangle$, σ' is the differential scattering cross section per steradian in the direction of the pump, and L is the length of the interaction region [30,32]. This yields $P_S^{th} \sim 1.2 \times 10^{-2}$, where $L = 70$ mm, the effective solid angle is $\Delta\Omega \sim 8.5 \times 10^{-3}$ for the collection optics, and the theoretical differential scattering cross section is $\sigma' = 1.2 \times 10^{-36}$ m^2 [30,33]. Including a fourth-power scaling of wavelength for the scattering cross section since $\sigma \propto \lambda_S^{-4}$ [32], the corresponding probability for anti-Stokes scattering is $P_A^{th} \approx \bar{n}(\lambda_S/\lambda_r)^4 P_S^{th} \sim 8.7 \times 10^{-4}$, where $\bar{n} = \exp(-h\nu/k_B T) = 0.06$ is the Boltzmann population weighting at $T = 295$ K, $\lambda_S = 845$ nm is the Stokes wavelength, and $\lambda_r = 805$ nm is the read pulse wavelength. We note that the measured detection rates are less than the estimated theoretical values due to imperfect avalanche photodiode (APD) detection efficiency, imperfect coupling to the fiber-coupled APDs, and losses from imperfect spectral filtering and polarization filtering. The low theoretical and measured scattering rates indicate that the scattering is spontaneous. This conclusion is further supported by the observed linear variation of the measured scattering probability with the write pulse energy. The probability that a single write or read pulse generates more than one photon is therefore small.

We verify the existence of nonclassical correlations between the Stokes and anti-Stokes photons by measuring their normalized intensity cross-correlation function,

$$g_{S,A}^{(2)} = \frac{P_{S,A}}{P_S P_A}, \quad (1)$$

where $P_{S,A}$ is the probability of a coincident Stokes and anti-Stokes detection. Figure 2 shows the measured

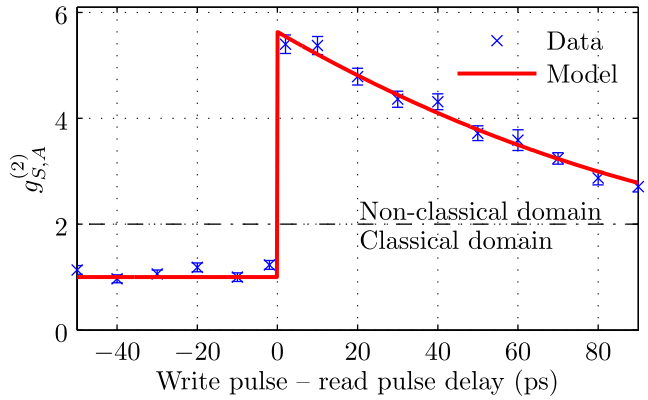

Fig. 2. Plot of measured $g^{(2)}_{S,A}$ as a function of write pulse–read pulse delay (blue cross). At positive delays $g^{(2)}_{S,A} > 2$, indicating nonclassical correlations between the detected Stokes and anti-Stokes photons. Standard errors are shown as error bars. A theoretical model shows close agreement with the measured values (solid red line).

intensity cross-correlation function $g^{(2)}_{S,A}(\tau)$ as a function of write–read pulse delay τ, with standard errors shown as error bars. At negative delays, $g^{(2)}_{S,A}(\tau < 0) \approx 1$; for positive delays, we measure a maximum value of $g^{(2)}_{S,A}(\tau = 2\ \text{ps}) = 5.4(2)$ before $g^{(2)}_{S,A}$ decays with a 1/e time of 78 ps. The correlations decay as a function of delay because collisions between the hydrogen molecules destroy the phase coherence of the DRQ created by the write pulse. Classically, the intensity cross-correlation function is bounded by the Cauchy–Schwarz inequality $g^{(2)}_{S,A} \le [g^{(2)}_{S,S} g^{(2)}_{A,A}]^{1/2}$, where $g^{(2)}_{S,S}$ and $g^{(2)}_{A,A}$ are the autocorrelation functions of the Stokes and anti-Stokes fields, respectively [34]. The Raman scattered fields are thermal, with single-mode theoretical values $g^{(2)}_{S,S} = g^{(2)}_{A,A} = 2$ [34]; measured values satisfying $g^{(2)}_{S,A} > 2$ therefore indicate nonclassical correlations between the fields. We measure values of $g^{(2)}_{S,A} > 2$ for delays of up to $\tau = 90$ ps, showing clear evidence of nonclassical correlations between the Stokes and anti-Stokes modes due to their coupling via a DRQ.

The detection probabilities can be modeled as a function of coupling constants and collection efficiencies [25]. We operate in the limit where the probability of scattering a single Stokes photon into the collection mode of the Stokes detector is small so that we can neglect low probability higher-order terms. The probabilities $P_S(P_A)$ for detecting a single Stokes (anti-Stokes) photon, or $P_{S,A}$ for a coincident detection, are then given by [25]

$$P_S = \eta_S P^{th}_S, \tag{2a}$$

$$P_A = \eta_A \beta\chi + \eta_A P^{th}_A, \tag{2b}$$

$$P_{S,A} = \eta_S \eta_A \alpha P^{th}_S + P_S P_A, \tag{2c}$$

where χ is the probability for a single Stokes photon to be scattered in any direction, β is the time-dependent probability that an anti-Stokes photon will scatter toward the collection optics from any DRQ created by the write pulse, α is the time-dependent probability that an anti-Stokes photon will scatter toward the collection optics given that a Stokes photon was detected, and $\eta_S(\eta_A)$ is the detection efficiency for photons in the Stokes (anti-Stokes) beam path.

We can evaluate $g^{(2)}_{S,A}$ by combining Eqs. (2a)–(2c) with $P^{th}_A \approx \bar{n}(\lambda_S/\lambda_r)^4 P^{th}_S$ to give

$$g^{(2)}_{S,A}(\tau \ge 0) = 1 + \frac{(\alpha_0/P^{th}_S)e^{-2\Gamma\tau}}{(\chi\beta_0/P^{th}_S)e^{-2\Gamma\tau} + \bar{n}(\lambda_S/\lambda_r)^4}, \tag{3}$$

where we have set

$$\alpha(\tau \ge 0) = \alpha_0 e^{-2\Gamma\tau}; \qquad \beta(\tau \ge 0) = \beta_0 e^{-2\Gamma\tau} \tag{4}$$

to account for the homogeneous damping effect of collisional dephasing at rate Γ on the DRQ created by the write pulse. The pressure-dependent dephasing rate is known to be $\Gamma_{18\,\text{bar}} = 0.645$ rad ns^{-1} from stimulated Raman gain spectroscopy [35]. Using (α_0/P^{th}_S) and $(\chi\beta_0/P^{th}_S)$ as free parameters we fit Eq. (3) to the measured data and obtain excellent agreement; the fit parameters are $(\alpha_0/P^{th}_S) = 0.46$ and $(\chi\beta_0/P^{th}_S) = 0.027$. Using the theoretical value for P^{th}_S, we estimate the retrieval efficiency of a DRQ heralded by the detection of a Stokes photon to be $\alpha_0 \sim 5.5 \times 10^{-3}$.

In conclusion, we have demonstrated quantum-level manipulations of THz-bandwidth photons using delocalized rotational quanta in a hydrogen ensemble at room temperature. We verified the existence of nonclassical Stokes–anti-Stokes correlations, measuring a maximum intensity cross-correlation value of $g^{(2)}_{S,A} = 5.4$. Noise and bandwidth limitations in many optical media render them unsuitable for use in ultrafast quantum photonic devices. This implementation of a fundamental building block for ultrafast photonic manipulations at the quantum level shows the promise of molecular states for quantum processing.

The authors wish to thank Khabat Heshami for helpful comments on the manuscript.

References

1. M. D. Eisaman, J. Fan, A. Migdall, and S. V. Polyakov, Rev. Sci. Instrum. **82**, 071101 (2011).
2. P. J. Bustard, D. Moffatt, R. Lausten, G. Wu, I. A. Walmsley, and B. J. Sussman, Opt. Express **19**, 25173 (2011).
3. P. Kok, W. J. Munro, K. Nemoto, T. C. Ralph, J. P. Dowling, and G. J. Milburn, Rev. Mod. Phys. **79**, 135 (2007).
4. D. F. Phillips, A. Fleischhauer, A. Mair, R. L. Walsworth, and M. D. Lukin, Phys. Rev. Lett. **86**, 783 (2001).
5. G. Hétet, J. J. Longdell, A. L. Alexander, P. K. Lam, and M. J. Sellars, Phys. Rev. Lett. **100**, 023601 (2008).
6. M. Afzelius, I. Usmani, A. Amari, B. Lauritzen, A. Walther, C. Simon, N. Sangouard, J. Minář, H. de Riedmatten, N. Gisin, and S. Kröll, Phys. Rev. Lett. **104**, 040503 (2010).
7. K. F. Reim, J. Nunn, V. O. Lorenz, B. J. Sussman, K. C. Lee, N. K. Langford, D. Jaksch, and I. A. Walmsley, Nat. Photonics **4**, 218 (2010).
8. A. Lvovsky, B. Sanders, and W. Tittel, Nat. Photonics **3**, 706 (2009).
9. A. E. Kozhekin, K. Mølmer, and E. Polzik, Phys. Rev. A **62**, 033809 (2000).
10. M. Fleischhauer and M. D. Lukin, Phys. Rev. A **65**, 022314 (2002).
11. H.-J. Briegel, W. Dür, J. I. Cirac, and P. Zoller, Phys. Rev. Lett. **81**, 5932 (1998).

12. N. Sangouard, C. Simon, H. de Riedmatten, and N. Gisin, Rev. Mod. Phys. **83**, 33 (2011).
13. M. D. Eisaman, A. André, F. Massou, M. Fleischhauer, A. S. Zibrov, and M. D. Lukin, Nature **438**, 837 (2005).
14. M. Hosseini, B. Sparkes, G. Hétet, J. Longdell, P. Lam, and B. Buchler, Nature **461**, 241 (2009).
15. C. Liu, Z. Dutton, C. H. Behroozi, and L. V. Hau, Nature **409**, 490 (2001).
16. B. Lauritzen, J. Minář, H. de Riedmatten, M. Afzelius, N. Sangouard, C. Simon, and N. Gisin, Phys. Rev. Lett. **104**, 080502 (2010).
17. C. Clausen, I. Usmani, F. Bussières, N. Sangouard, M. Afzelius, H. de Riedmatten, and N. Gisin, Nature **469**, 508 (2011).
18. E. Saglamyurek, N. Sinclair, J. Jin, J. A. Slater, D. Oblak, F. Bussières, M. George, R. Ricken, W. Sohler, and W. Tittel, Nature **469**, 512 (2011).
19. A. Alexander, J. Longdell, M. Sellars, and N. Manson, J. Lumin. **127**, 94 (2007).
20. M. Hedges, J. Longdell, Y. Li, and M. Sellars, Nature **465**, 1052 (2010).
21. P. J. Bustard, R. Lausten, D. G. England, and B. J. Sussman, Phys. Rev. Lett. **111**, 083901 (2013).
22. L.-M. Duan, M. D. Lukin, J. I. Cirac, and P. Zoller, Nature **414**, 413 (2001).
23. C. H. van der Wal, M. D. Eisaman, A. André, R. L. Walsworth, D. F. Phillips, A. S. Zibrov, and M. D. Lukin, Science **301**, 196 (2003).
24. D. N. Matsukevich, T. Chanelière, S. D. Jenkins, S.-Y. Lan, T. A. B. Kennedy, and A. Kuzmich, Phys. Rev. Lett. **97**, 013601 (2006).
25. S. Chen, Y.-A. Chen, T. Strassel, Z.-S. Yuan, B. Zhao, J. Schmiedmayer, and J.-W. Pan, Phys. Rev. Lett. **97**, 173004 (2006).
26. M. Bashkansky, F. K. Fatemi, and I. Vurgaftman, Opt. Lett. **37**, 142 (2012).
27. A. Kuzmich, W. Bowen, A. Boozer, A. Boca, C. Chou, L.-M. Duan, and H. Kimble, Nature **423**, 731 (2003).
28. K. C. Lee, B. J. Sussman, M. R. Sprague, P. Michelberger, K. F. Reim, J. Nunn, N. K. Langford, P. J. Bustard, D. Jaksch, and I. A. Walmsley, Nat. Photonics **6**, 41 (2011).
29. G. Herzberg, *Molecular Spectra and Molecular Structure* (Van Nostrand, 1950), Vol. **1**.
30. D. A. Long, *The Raman Effect: A Unified Treatment of the Theory of Raman Scattering by Molecules* (Wiley, 2002).
31. R. W. Minck, E. E. Hagenlocker, and W. G. Rado, Phys. Rev. Lett. **17**, 229 (1966).
32. A. Penzkofer, A. Laubereau, and W. Kaiser, Prog. Quant. Electron. **6**, 55 (1979).
33. K. J. Miller, J. Am. Chem. Soc. **112**, 8543 (1990).
34. R. Loudon, *The Quantum Theory of Light* (Oxford University, 2004).
35. G. C. Herring, M. J. Dyer, and W. K. Bischel, Phys. Rev. A **34**, 1944 (1986).